J. Chem. Sci. (2018) 130:115
https://doi.org/10.1007/s12039-018-1522-4

REGULAR ARTICLE

Density functional theory studies on PVDF/ionic liquid composite systems

RANJINI SARKAR and T K KUNDU*
Department of Metallurgical and Materials Engineering, Indian Institute of Technology Kharagpur, Kharagpur, West Bengal 721 302, India
E-mail: tkkundu@metal.iitkgp.ac.in

MS received 19 January 2018; revised 25 May 2018; accepted 12 June 2018; published online 3 August 2018

Abstract. Density functional theory calculations with and without dispersion correction were performed to describe the effect of the addition of ionic liquids (ILs) to polyvinylidene fluoride (PVDF) molecules. All the calculations were carried out for four monomer units of α- and β-PVDF and 1-n-alkyl 3-methylimidazolium tetrafluoroborate [C_nMIM] [BF_4] (n = 2, 4, 6, 8, 10) ionic liquids. Dispersion correction is found to be essential to describe ion pair (within the IL molecule) interaction and polymer–ionic liquid interaction. Frontier orbitals (HOMO, LUMO) compositions and energies were obtained for individual PVDF molecules, ionic liquids and ionic liquid added polymer complexes to demonstrate the variation in different chemical parameters like hardness, softness, chemical potential, electronegativity, the electron affinity of the systems. Mulliken and atomic dipole moment corrected Hirschfeld population analyses were carried out to provide a quantitative analysis of partial atomic charge distribution. Molecular electrostatic potential plots, mapped on to total electron density surfaces, are provided to depict the reactive parts of the molecules under study. Natural bond orbital analysis was also carried out to quantify the extent of electron delocalization caused by PVDF–IL anion and PVDF–IL cation weak interactions.

Keywords. Dispersion-corrected DFT; interaction energy; HOMO–LUMO; molecular electrostatic potential; natural bond orbital; PVDF–ionic liquid.

1. Introduction

Five distinct polymorphs (α, β, γ, δ and ε) of polyvinylidene fluoride (PVDF) can be formed depending on the crystallization conditions and processing techniques.[1–3] Among these, β and γ forms are polar (show piezoelectric and ferroelectric properties) and the rest are non-polar.[4] However, β-PVDF is of immense technological importance because of its higher dipole moment and, consequently, higher spontaneous polarization per monomer unit.[5] This conformation possesses a dipole density value[4] of 0.18 C/m^2 which is comparable with the dipole density value of 0.26 C/m^2 corresponding to the most discussed ferroelectric, $BaTiO_3$.[6] Electroactive polymers are easy to fabricate and to some extent more advantageous as compared to electroactive ceramics because of their (polymers) low density (1000–2000 kg/m^3), flexibility, high response speed (μ to min), better resilience, and higher actuation strain.[7] β-PVDF is found to possess low dielectric constant, elastic stiffness and acoustic impedance[8] which make it potential sensor material with high voltage sensitivity. Besides, among all the ferroelectric polymers, β-PVDF exhibits the highest Curie temperature of 168 °C and very high coercive electric field of 120 MV/m at room temperature.[9] In spite of all these advantages, β-PVDF is associated with a major disadvantage of its structural instability.[10] Among all the conformations of PVDF, α-phase possesses the highest stability and therefore it is formed predominantly during melting or solvent casting.[11] Wang *et al.*,[10] calculated that β to α transformation is thermodynamically more spontaneous (the energy barrier for α to β transition is 16.3 kJ/mol whereas the same for β to

*For correspondence

Electronic supplementary material: The online version of this article (https://doi.org/10.1007/s12039-018-1522-4) contains supplementary material, which is available to authorized users.

α transition is 8.2 kJ/mol). However, Gomes *et al.,*[12] quantitatively determined that ferroelectric switching conditions of PVDF are inherently dependent on the β-phase content. This fact instigated a search for new synthesis strategies of β-PVDF. Formation of β-PVDF may follow two paths:[13] a) direct synthesis or b) conversion of α to β conformation. Previously, mechanical stretching and electrical poling along with various high temperature–high pressure treatments were used to be carried out on the non-polar α-PVDF polymer chain to promote crystallization of polar β-PVDF phases.[12,14,15] Interestingly, the addition of different types of second phase materials also helps in improving the fractional content of β-PVDF from the PVDF blend and thereby enhancing the electrical properties. 0–3 type ferroelectric nanocomposites are synthesized with ferroelectric ($BaTiO_3$, $Ba_{0.5}Na_{0.5}TiO_3$, La_2O_3, PZT, $BaSrTiO_3$, $PbTiO_3$, $BaFe_{0.5}Nb_{0.5}O_3$)[16–22] nanoparticles as the second phase in the PVDF matrix. This type of composites exploits the properties of both the ferroelectric nanofillers and electroactive β-PVDF polymer resulting in large spontaneous polarization, enhanced dielectric constant and improved piezo- and pyroelectric properties. The strong electrostatic interaction between positive ($-CF_2$) dipole moment of the PVDF polymer chain and the negative surface of the nanoparticles; hydrogen bonding interaction between PVDF and the second phase materials are found to be the main reasons behind the improvement of the crystallization kinetics of β-PVDF resulting in improved ferroelectric and dielectric properties. Similar kind of strong interaction is found in PVDF thin films modified with hydrated salts, e.g., $Ce(NO_3)_3{\cdot}9H_2O$, $Y(NO_3)_3{\cdot}9H_2O$.[23] Addition of different room temperature ionic liquids (RTILs) into PVDF blend is reported as another method, which promotes crystallization of electroactive β phase as a result of strong electrostatic interaction between dipole moments of β-PVDF and ionic liquids.[24,25] Ionic liquids are comprised of heterocyclic cations and small anions with high chemical stability, high ionic conductivity and infinitesimally small vapor pressure at operating temperature.[24–26] They show good miscibility within PVDF matrix, work as plasticizer and improve the optical, electrical and mechanical properties of the polymer.[26] PVDF/IL composites are found to exhibit excellent ductility, good optical transparency, enhanced ionic conductivity, and high dielectric constant[27] which increase their applicability in the field of high performance piezoelectric sensors, actuators and energy storage materials. This fact instigated the necessity of theoretical analysis of this kind of systems. According to the experimental observations, the addition of very less amount of ionic liquid to pristine PVDF system, which is predominantly in non-polar α phase, helps in crystallisation of β-PVDF. But to the best of the author's knowledge, this phenomenon lacks theoretical explanation. The current article intends to provide a detailed quantum chemical description of PVDF/IL molecular complexes using density functional theory calculations, which has been successful in analysing the structure, stability and electronic properties for this type of chemical systems.[28,29] To identify the exact regions of molecular interaction it is important to consider the PVDF and ionic liquid molecules as isolated systems. Both α- and β-PVDF are studied in the pure state, as well as in PVDF/IL complex state to provide a comparative analysis of the molecular interaction. All the calculations are carried out for four monomer units of α and β-PVDF molecules and the ionic liquids having tetrafluoroborate anion [BF_4] and methylimidazolium-based cation with an alkyl group present at 1-C position [C_nMIM]. The alkyl chain (attached to the imidazolium ring) length of the IL cation is varied from 2 to 10, forming 1-ethyl-3-methylimidazolium tetrafluoroborate ([C_2MIM][BF_4]), 1-butyl-3-methylimidazolium tetrafluoroborate ([C_4MIM][BF_4] or [BMIM][BF_4]), 1-hexyl-3-methylimidazolium tetrafluoroborate ([C_6MIM][BF_4]), 1-octyl-3-methylimidazolium tetrafluoroborate ([C_8MIM][BF_4]) and 1-decyl-3-methylimidazolium tetrafluoroborate ([C_{10}MIM][BF_4]), to examine the effect of increasing cation size of the ionic liquids on PVDF/IL complex systems.

2. Computational details

All the density functional theory calculations are carried out in the Gaussian09[30] program in the gas phase model by a linear combination of atomic orbitals (LCAO) approach using Gaussian-type basis sets.[31] Initially, different density functional with and without dispersion correction, and basis sets are considered for geometry optimization of the base molecules (α and β-PVDF with four monomer units) to find the proper functional and basis set for subsequent calculations of the PVDF/IL systems. Grimme's dispersion-corrected DFT method (DFT-D)[32] has been found to be very effective for simulating the complex molecules as it takes into account the intra and inter-unit interaction by incorporating a dispersion correction factor into the total energy term as obtained from standard density functional calculations, expressed as follows,

$$E_{DFT-D} = E_{DFT} + S\sum_{i\neq j}\frac{C_{ij}}{r_{ij}^6} f_{damp}\left(r_{ij}\right) \quad (1)$$

where, r_{ij} is the distance between atoms 'i' and 'j', C_{ij} is the dispersion coefficient for atoms 'i' and 'j', $f_{damp}\left(r_{ij}\right)$ is a damping function to avoid unphysical behavior of the dispersion term at small distances and S is the scaling factor

applied uniformly to all pairs of atoms. Among the 'standard functionals' (without dispersion) Becke's non-local gradient-corrected three parameter exchange functional[33] with two correlation functional, as developed by Lee-Yang-Parr[34] (named as B3LYP) and another by Perdew-Wang[35] (named as B3PW91) are used with three types of basis sets, 6-31+G(d,p), 6-311+G(d,p) and 6-311++G(d,p). Dispersion-corrected calculations are performed using 6-311+G(d,p) basis set and standard B3LYP functional (with 'dft-d' keyword), as well as using dispersion-corrected density functionals, namely, M06-2X[36] and WB97XD.[37]

Interaction energy (ΔE) values[28,38] of PVDF/IL complexes are obtained using the following expression,

$$\Delta E = E_{PVDF+IL} - (E_{PVDF} + E_{IL}) \tag{2}$$

where, $E_{PVDF+IL}$ = energy of optimized ionic liquid added β-PVDF molecule, E_{PVDF} = energy of optimized pure β-PVDF molecule and E_{IL} = energy of the optimized pure ionic liquid molecule.

Intra- and inter-unit energetic interactions within the systems under study are characterized by natural bond orbital (NBO) analysis,[39] carried out in NBO 3.1 program implemented in Gaussian09 package, which quantifies the loss of electron density (electron delocalization) in the donor (Lewis) NBOs into empty acceptor (non-Lewis) NBOs during interaction, resulting in significant departure from the idealized Lewis structures. The extent of electron delocalization is proportional to the stabilization energy ($E^{(2)}$) associated with i (donor) → j (acceptor) delocalization and is mathematically defined using the second order perturbation theory as follows,

$$E^{(2)} = \Delta E_{ij}^{(2)} = \frac{q_i F(i,j)^2}{\varepsilon_j - \varepsilon_i} \tag{3}$$

where, q_i is donor orbital occupancy; ε_i, ε_j are diagonal elements of the Fock matrix; F (i, j) are the off-diagonal elements of the Fock matrix.

Partial atomic charge distribution within the systems under study is demonstrated using two types of charge population analysis schemes, a) Mulliken population analysis (MPA) and b) Hirschfeld population analysis (HPA). MPA[40] provides a means of estimating partial atomic charges from calculations carried out by the methods involving a linear combination of atomic orbital molecular orbital (LCAO MO) theory. However, the major disadvantage of this population analysis scheme is its high basis set dependence and therefore less reliability compared to HPA method, which is based on deformation density partition.[41] But Hirschfeld atomic charges are too small and have a poor reproducibility of the observable quantities as it ignores atomic dipole moments. Therefore, atomic dipole moment corrected Hirschfeld (ADCH) population analysis[42] is also carried out, where, Hirschfeld charges are corrected by expanding atomic dipole moments to correct charges placed at neighbouring atoms. In the current study, HPA and ADCHPA are carried out in Multiwfn program.[43]

Dipole moment and polarizability are two important properties to characterize a piezoelectric material. The dipole moment is the first derivative of energy with respect to an applied electric field. It is the measure of the asymmetry in the molecular charge distribution and is given as a vector in three dimensions (X, Y and Z) as μ_x, μ_y and μ_z, respectively. And molecular polarizability is quantified as the second derivative of the energy of the molecule with respect to an electric field. Net dipole moments (μ_0) and mean polarizabilities (α_0) are calculated from the dipole moment vectors (μ_x, μ_y, μ_z) and molecular exact polarizability tensors (α_{xx}, α_{yy}, α_{zz}) according to the following mathematical formulae,[44]

$$\mu_0 = \left(\mu_x^2 + \mu_y^2 + \mu_z^2\right)^{\frac{1}{2}} \tag{4}$$

$$\alpha_0 = \frac{1}{3}\left(\alpha_{xx} + \alpha_{yy} + \alpha_{zz}\right) \tag{5}$$

Frontier orbitals (highest occupied molecular orbital (HOMO) and lowest unoccupied molecular orbital (LUMO) energies of a molecule can be directly correlated to different chemical parameters which provide thorough insight to the reactivity and selectivity of it. According to Koopmans' theorem[45] for closed-shell systems, ionization potential IP=-HOMO energy and electron affinity EA=-LUMO energy. Using finite approximation for the small change in the number of particles, different physical and chemical parameters can be evaluated from these HOMO–LUMO energy values[46–48] as given below:

$$\text{Electronegativity } (\chi) = \frac{IP + EA}{2} \tag{6}$$

$$\text{Chemical potential } (\mu) = -\left(\frac{IP + EA}{2}\right) \tag{7}$$

$$\text{Chemical hardness } (\eta) = \frac{IP - EA}{2} \tag{8}$$

$$\text{Chemical softness } (S) = \frac{1}{\eta} \tag{9}$$

$$\text{Electrophilicity index } (\omega) = \frac{\left(\frac{IP+EA}{2}\right)^2}{IP - EA} = \frac{\mu^2}{2\eta} \tag{10}$$

To elucidate the effects of ionic liquids as a solvent on the PVDF system, simulation of an individual β-PVDF molecule within [C_4MIM][BF_4] solvent continuum is carried out using the solvation model based on density (SMD) computational approach.[49] The key descriptors of ionic liquid [C_4MIM][BF_4] used in the calculations, as obtained by Bernales *et al.*,[50] are provided below.

Solvent dielectric constant = 11.70
Index of refraction (n) = 1.4215
Macroscopic surface tension (γ) = 67.07
Abraham's hydrogen bond acidity parameter when treated as a solute ($\sum \alpha_2^H$) = 0.263
Abraham's hydrogen bond basicity parameter when treated as a solute ($\sum \beta_2^H$) = 0.320
The fraction of non-hydrogen atoms that are aromatic carbon atoms (φ) = 0.2

The fraction of non-hydrogen atoms that are electronegative halogen atoms (ψ) = 0.2667

3. Results and Discussion

3.1 *Geometry optimization*

Four monomer units of α- and β-PVDF and five derivatives of methylimidazolium tetrafluoroborate ionic liquid, as mentioned in Section 1, have been optimized using various DFT methods. Optimized structures of α-PVDF, β-PVDF and [C_{10}MIM][BF_4] are presented in Figures 1 (a), (b) and (c), respectively. Rest of the ILs under study, i.e., [C_nMIM] [BF_4], [n=2, 4, 6, 8, 10] are given in Supplementary Figure S1 (a)–(e) and their energy values are provided in Supplementary Table S2. α-PVDF (with C_1 symmetry) is found to possess lower energy than β-PVDF (with C_S symmetry) ensuring the higher stability of the former, as given in Table 1, where relative energy, dipole moment (per monomer unit) and mean polarizability (per monomer unit) values are presented for α and β-PVDF for different calculation methods. β-PVDF possesses all trans (TTTT) configuration where all the fluorine atoms (and hydrogen atoms) are situated on the same side of the polymer backbone chain, resulting in a similar type of atomic repulsion. This high repulsive energy within β-PVDF molecule results in less stability than α-PVDF which exhibits trans-gauche (TGTG') configuration containing pairs of fluorine and hydrogen atoms at the alternative sides of the PVDF backbone chain. Besides, frequency calculations on optimized structures of β-PVDF generate three imaginary frequencies (as given in supplementary Table S1), although too small to consider in case of all the density functional methods mentioned here. This also suggests the structural instability of β-PVDF. However, B3LYP with dft-d calculation using 6-311+G(d,p) basis set is found to give the lowest energy configuration for both α and β-PVDF (Table 1). Optimized structures of PVDF/IL complex molecules are found to become more stable with the increase in their size. Dispersion correction in DFT methods is demonstrated for α-PVDF/[C_{10}MIM][BF_4] and β-PVDF/[C_{10}MIM][BF_4] structures in Figures 2 and 3 (rest of the α-PVDF/IL and β-PVDF/IL optimized structures are shown in Supplementary Figures S2(a)–(e) and Figure S3(a)–(e), respectively) which show that when long-range dispersion phenomenon is taken into account, the relative distances between different units (anion and cation of the ionic liquids, and PVDF) of the PVDF/IL complexes reduce significantly. But the magnitudes of the resultant dipole moment vector of β-PVDF/IL molecules are found to be lower than that of

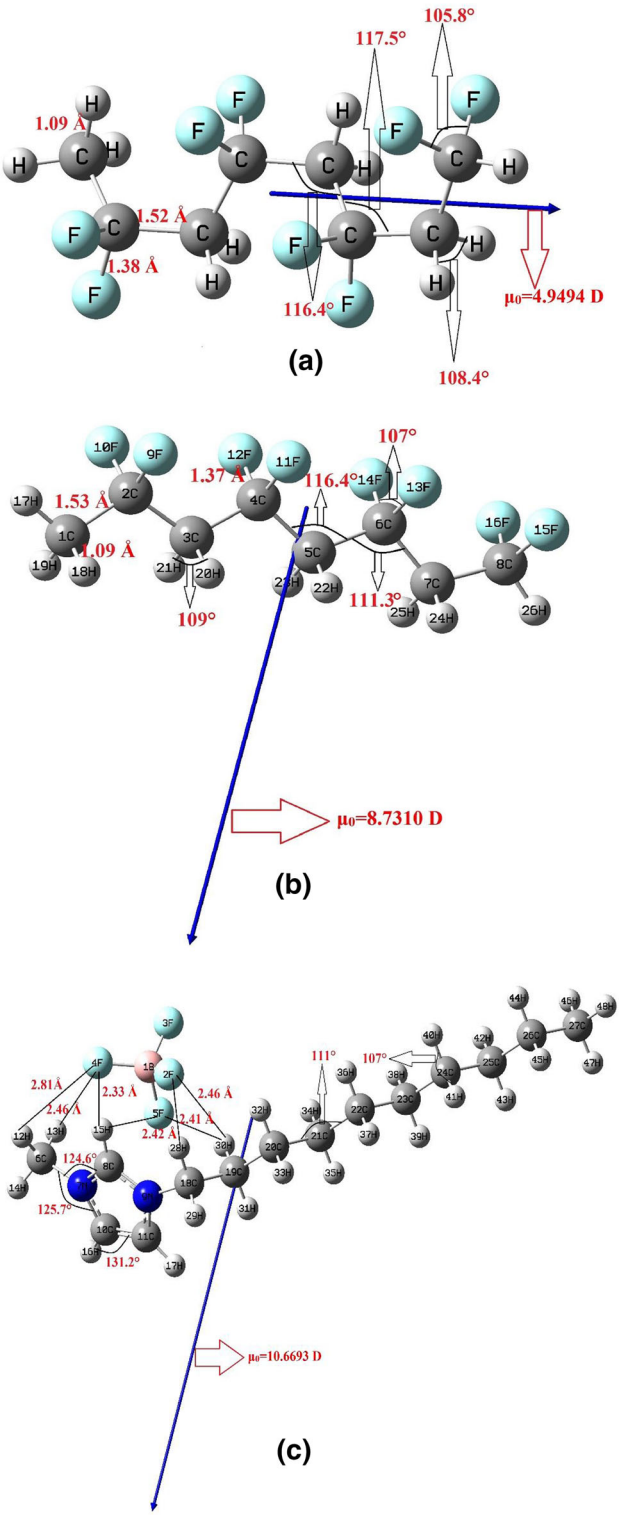

Figure 1. Optimized structures of (a) α-PVDF, (b) β-PVDF, (c) [C_{10}MIM][BF_4], showing average bond lengths, bond angles, cation-anion distances (for ionic liquid) and dipole moment vectors (μ_0) [method: DFT-D; functional: B3LYP; basis set: 6-311+G(d,p)].

α-PVDF/IL molecules. This evidently supports better ion–dipole interaction within β-PVDF/IL than within α-PVDF/IL molecules. As dispersion corrected B3LYP

Table 1. Relative energy differences (reference method: B3LYP-D functional and 6-311+G(d,p) basis set), dipole moment and polarizability values corresponding to the optimized structures of α and β-PVDF obtained from different functional and basis sets.

Method, Functional, Basis Set	α-PVDF (C_1 point group symmetry)			β-PVDF (C_S point group symmetry)		
	$E\text{-}E_{ref,\alpha}$ (kJ/mol) [$E_{ref,\alpha}$ = − 1110.026 a.u]	Dipole moment per monomer unit (C-m) [Expt value* = 4.00E–30]	Polarizability per monomer unit (cm^2/V) [Expt value*= 3.56E−40]	$E\text{-}E_{ref,\beta}$ (kJ/mol) [$E_{ref,\beta}$ = -1110.012 a.u]	Dipole moment per monomer unit (C-m) [Expt value* = 7.00E−30]	Polarizability per monomer unit (cm^2/V) [Expt value*= 3.63E−40]
DFT-D, B3LYP, 6-311+G(d,p)	0	4.13E-30	4.03E-40	0	7.28E-30	4.10E-40
B3LYP, 6-31+G(d,p)	843.65	4.15E-30	4.09E-40	835.21	7.19E-30	4.15E-40
B3LYP, 6-311++G(d,p)	103.32	4.2E-30	4.07E-40	95.44	7.29E-30	4.13E-40
B3PW91, 6-31+G(d,p)	1934.74	4.04E-30	4.04E-40	1924.89	7.02E-30	4.10E-40
B3PW91, 6-311++G(d,p)	1212.13	4.07E-30	4.01E-40	1202.87	7.12E-30	4.08E-40
WB97XD, 6-311+G(d,p)	1705.10	4.1E-30	3.95E-40	918.25	7.20E-30	4.01E-40
M06-2X, 6-311+G(d,p)	1112.36	4.13E-30	3.86E-40	1110.92	7.29E-30	3.13E-40

Experimental values are taken from ref.[51].

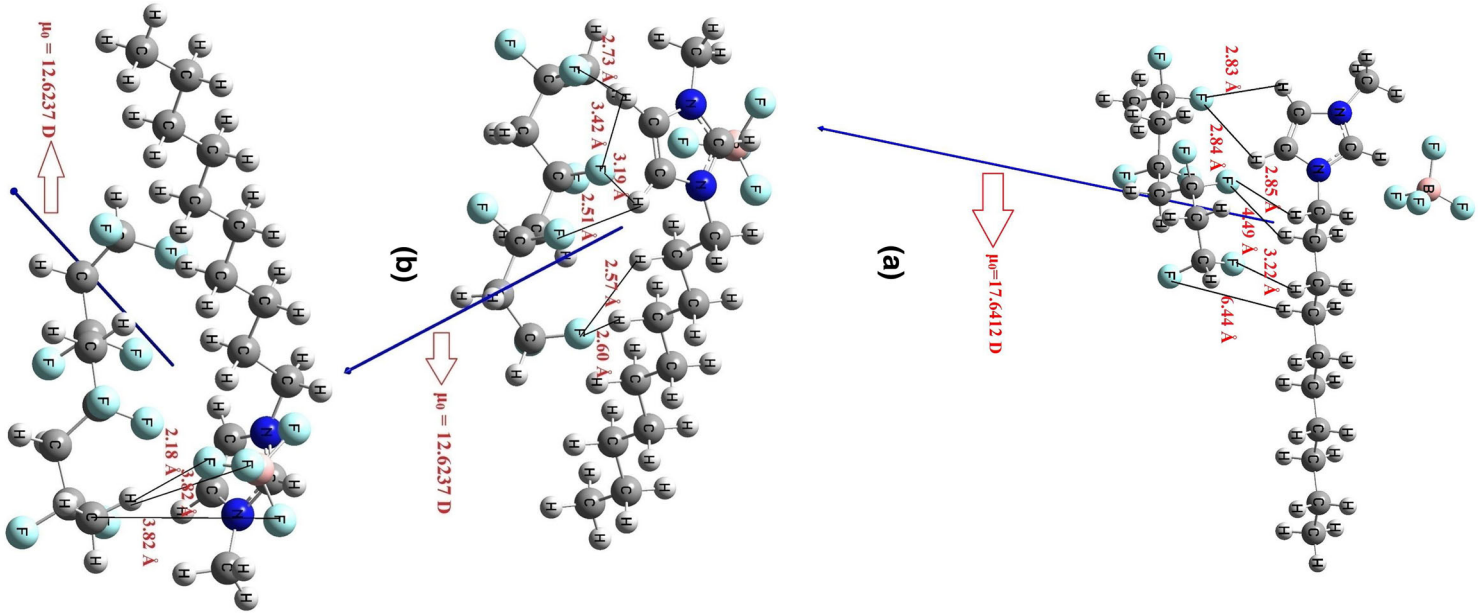

Figure 2. Optimized structure of α-PVDF/[C_{10}MIM][BF_4]. (a) without dispersion correction [functional: B3LYP; basis set: 6-31+G(d,p)], (b) with dispersion correction showing average cation-PVDF distances [method: DFT-D; functional: B3LYP; basis set: 6-311+G(d,p)], (c) with dispersion correction showing average anion-PVDF distances [method: DFT-D; functional: B3LYP; basis set: 6-311+G(d,p)].

functional and 6-311+G(d,p) basis set are found to take this inter-unit interaction into account most effectively (as it produces the least energy structures according to Table 1), subsequent calculations are carried out using this functional and basis set only.

Different structural parameters of β-PVDF before and after ionic liquid addition are provided in Table 2. Calculated structural parameters of pure α and β-PVDF, obtained from aforementioned simulation method, match well with experimental values as reported in Ref.[51] After ionic liquid addition, the PVDF structure changes from C_S to C_1 symmetry which is evident from the dihedral angle values. But no considerable change is observed in the intra-unit bond length and bond angles of the molecular complexes.

3.2 *Interaction energy calculation*

The interaction energies of PVDF/ionic liquid complexes under study are calculated according to equation 2 and provided in Table 3 which shows that all the $[C_nMIM][BF_4]$ ionic liquids possess negative interaction energy with both α and β-PVDF. A positive interaction energy value signifies a stronger bond within the isolated molecules of a complex but negative value of interaction energy indicates favourable interaction within them.[52] Magnitudes of interaction energies of ionic liquid molecules with β-PVDF are found to be significantly more negative than that with α-PVDF. This can be a suitable justification of the increase in the fractional content of electroactive β-PVDF crystals in the PVDF blend after ionic liquid addition, as mentioned previously. This is because the electrostatic interaction of the negative charge of ionic liquid anions with the positive side of the PVDF dipole moments which results in preferential orientation of the polymer chain in the all trans (β) configuration.[53,54] However, $[C_{10}MIM][BF_4]$ results in the best favourable interaction with α- and β-PVDF among all the ionic liquids discussed here.

3.3 *Dipole moment and polarizability*

Calculated net dipole moment and mean polarizability of per monomer unit of α- and β-PVDF using different DFT methods are provided in Table 1, which show that all the methods show satisfactory agreement with the experimental results.[54] Molecular dipole moment and polarizability values of optimized structures of pure β-PVDF, pure IL and β-PVDF/IL complexes, with and without dispersion correction, are provided in supplementary Table S2 and the direction of the dipole moment vectors for α-PVDF, β-PVDF, $[C_{10}MIM][BF_4]$, α-PVDF/$[C_2MIM][BF_4]$ and β-PVDF/$[C_{10}MIM][BF_4]$ are shown in Figures 1, 2 and 3. Evidently, computed values of dipole moment and polarizability of β-PVDF/IL systems are found as higher than that of α-PVDF/IL systems without considering dispersion. On the contrary, ionic liquid added α-PVDF is found to exhibit higher dipole moment than ionic liquid added β-PVDF molecules in case of DFT-D calculations (Table S2, Supplementary Information). This is because taking into account high dipolar interaction between ionic liquid and β-PVDF in the calculations makes the optimized structures more compact, which further reduces the net dipole moment. However, the magnitudes of dipole moments of PVDF/IL molecules are almost independent of the alkyl chain-length in the cation of ionic liquid in case of both standard and dispersion-corrected DFT calculations. But mean polarizability values of all the systems increase with the increase in the alkyl chain length of the attached to the imidazolium ring present in the cation of the ionic liquids.

3.4 *Population analysis*

Mulliken and Hirschfeld population analyses have been carried out for a pristine β-PVDF molecule using different functional and basis sets to provide a comparative description of the two population analysis schemes (Table S3, Supplementary Information). As mentioned in Section 2, HPA is found to be basis set independent. The change in atomic dipole moment corrected Hirschfeld (ADCH) charge distribution within β-PVDF molecule after the ionic liquid addition is shown in Table 4 (Complete ADCH population analysis performed for all β-PVDF/IL systems under study are presented in Table S4, Supplementary Information). Within the β-PVDF molecule, all the fluorine atoms (F9-16*) and the carbon atoms bonding with the hydrogen atom pairs (C1, C3, C5, C7*) contain negative partial charges i.e., they are potential electron acceptors. On the other hand, all the hydrogen atoms (H17-26) and the carbon atoms bonding with fluorine atom pairs possess (C2, C4, C6, C8*) positive atomic charges and act as electron donors (Table 4) (refer to Figure 1 and Figure 3(b) for atom numbers). This explains the higher electronegativity of F atoms in C-F bonds and lower electronegativity of H atoms in C-H bonds. No significant change in population is observed within β-PVDF part of PVDF/IL complexes with the change in alkyl chain length of the IL cation. But a larger variation on a charge is observed in the ionic liquid portion of the complex molecules, suggesting higher chemical reactivity of ILs. The highest positive charge is accumulated within the boron atom (B27*) present in the $[BF_4]$ IL anion and H42*, H43* atoms in the IL cation. The highest

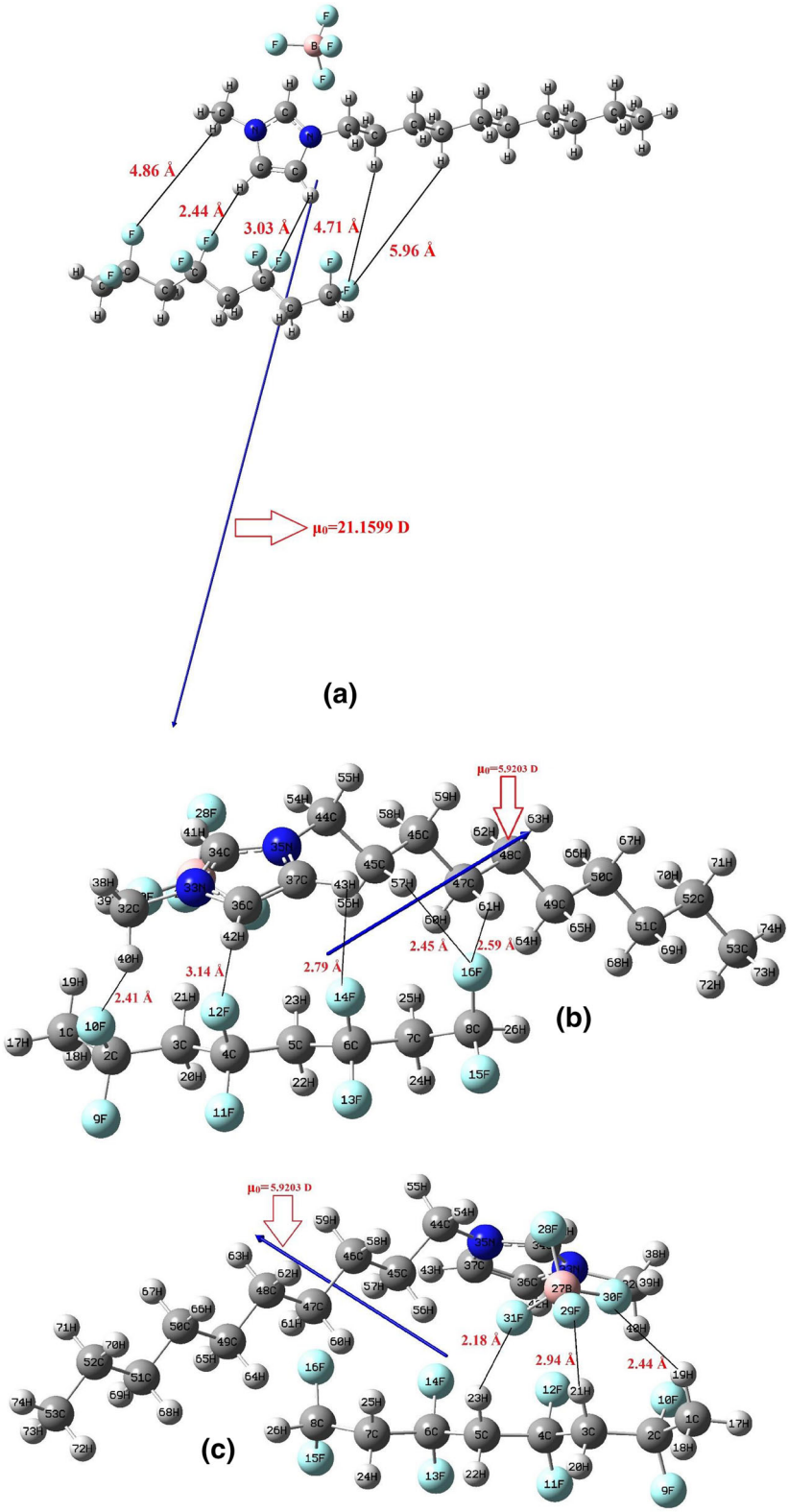

Figure 3. Optimized structure of β-PVDF/[C_{10}MIM][BF_4]. (a) without dispersion correction [functional: B3LYP; basis set: 6-31+G(d,p)], (b) with dispersion correction showing average cation-PVDF distances [method: DFT-D; functional: B3LYP; basis set: 6-311+G(d,p)], (c) with dispersion correction showing average anion-PVDF distances [method: DFT-D; functional: B3LYP; basis set: 6-311+G(d,p)].

negative charge is found to be accumulated within the fluorine atoms present in the anion and the C36*, *C37** atoms (Table S4, Supplementary Information) within IL cation.

3.5 *Frontier orbitals, their composition analysis and chemical parameters*

The positions and distribution of frontier orbitals, i.e., HOMO and LUMO in β-PVDF, [C_2MIM] [BF_4], β-PVDF/[C_2MIM][BF_4] are shown in Figure 4, and that in [C_{10}MIM][BF_4], β-PVDF/[C_{10}MIM][BF_4] are shown in Figure 5 (refer Figures S4 and S5 (Supplementary Information) for the remaining systems under study). The HOMO and LUMO compositions of all the atoms present in the molecules are calculated with Hirschfeld orbital composition analysis[55] algorithm using Multiwfn program.[43] This orbital composition method is reliable because of its high basis set stability. Figure 4(a) shows that the positions of HOMO and LUMO in pure β-PVDF is spread almost over the entire molecule, which is verified by the orbital composition analysis as given in Table 5. The orbitals of carbon and fluorine atoms contribute more to HOMO than that of hydrogen atoms in the system, whereas the hydrogen atom pairs attached to the polymer backbone chain contribute more to the LUMO composition. In case of both HOMO and LUMO, fluorine and hydrogen atoms within an atom pair possess equal contribution (Table 5) which infers the structural symmetry of the molecule. In case of pure ionic liquids, LUMO is mainly concentrated within the imidazolium ring of the cations, where HOMO is extended over a considerable portion of both cation and anion parts of the molecules, as shown in Figure 4(b) and Figure 5(a). According to Figure 4(c) and Figure 5(b), in ionic liquid added β-PVDF molecules, both HOMO and LUMO shift entirely to the ionic liquid part (specifically the imidazolium ring in the cation), which infers higher chemical reactivity of the ionic liquids. The HOMO-concentrated parts of the molecules tend to have high electron-donating capacity whereas the LUMO-concentrated sites possess high electron accepting capacity.[29] The atomic compositions corresponding to the maximum contribution (>5%) to the HOMO and LUMO of ionic liquid added β-PVDF systems are listed in Tables 6 and 7, respectively. For every ionic liquid added β-system, the imidazolium rings of the cations of ionic liquids comprised of three carbon atoms C34, C36†, C37† and two nitrogen atoms N33†, N35† cover almost 88% of total HOMO composition and atoms N33†, C34†, N35†, C71† and H41† cover almost around 75% of total LUMO composition († refer Figure 3(b)

Table 2. Structural parameters of pure and ionic liquid added β-PVDF [calculation method: DFT-D, functional used: B3LYP, basis set: 6-311+G(d,p)].

Structural parameters*		Name of the molecule						
		α-PVDF with C_1 symmetry	β-PVDF with C_S symmetry	β-PVDF/ [C_2MIM][BF_4]	β-PVDF/ [C_4MIM][BF_4]	β-PVDF/ [C_6MIM][BF_4]	β-PVDF/ [C_8MIM][BF_4]	β-PVDF/ [C_{10}MIM][BF_4]
Bond length (Å)	d_{C-F}	1.38{1.34}	1.37 {1.34}	1.378	1.3777	1.3777	1.377	1.377
	d_{C-H}	1.09{1.09}	1.09 {1.09}	1.0915	1.0914	1.0927	1.0914	1.0914
	d_{C-C}	1.52{1.54}	1.53 {1.54}	1.522	1.522	1.522	1.522	1.522
Bond angle (degree)	$\angle C_F - C_H - C_F$	116.4{116.5}	117.6 {112.5}	117.30	117.84	117.92	117.99	117.83
	$\angle C_H - C_F - C_H$	117.5 {118.5}	111.3 {112.5}	111.458	111.16	111.13	111.07	111.20
	∠F-C-F	105.8 {103}	106.9{108}	106.06	106.09	106.08	106.08	106.09
	∠H-C-H	108	108.8{112}	108.59	108.64	108.50	108.52	108.51
Dihedral angle (degree)	C-C-C-C	171, 49{179,45}**	180	168.05	172.86	173.50	173.80	173.58

*Structural parameters: d_{C-C}= average distance between two adjacent C atoms present in the PVDF backbone, d_{C-F}= average distance between the C and F atoms within a C-F-C pair, d_{C-H}= average distance between C and H atoms within a C-H-C pair, $\angle C_F - C_H - C_F$ and $\angle C_H - C_F - C_H$= angle between two adjacent C-C bonds, C_F represents the C atoms bonding with two F atoms and C_H refers to the C atoms bonding with two H atoms, ∠F-C-F= angle between two C-F bonds, ∠H-C-H= angle between two C-H bonds and C-C-C-C = dihedral angle constituted by four adjacent C atoms of the PVDF backbone chain.** two dihedral angle values for TGTG' confirmation

***Note: experimental values are given within {} bracket and taken from Ref.*[51]**

Table 3. Energy of interaction of α and β-PVDF molecules with ionic liquids [computation method: DFT-D; functional: B3LYP; basis set: 6-311+G(d,p)].

Name of ionic liquid	Energy of interaction (ΔE) with PVDF molecules (kJ/mol)		
	Interaction with α-PVDF	Interaction with β-PVDF	
		β-PVDF with C_S symmetry	β-PVDF with C_1 symmetry
$[C_2MIM][BF_4]$	−43.4995	−115.562	−112.819
$[C_4MIM][BF_4]$	−46.6658	−118.498	−115.755
$[C_6MIM][BF_4]$	−47.8631	−121.107	−118.363
$[C_8MIM][BF_4]$	−47.5626	−121.022	−118.278
$[C_{10}MIM][BF_4]$	−66.4333	−121.254	−118.51

Table 4. ADCH population analysis of the atoms present in β-PVDF molecules before and after ionic liquid addition (refer Figure 1(b) for atom numbers).

Atom number	Pure β-PVDF	β-PVDF/ $[C_2MIM][BF_4]$	β-PVDF/ $[C_4MIM][BF_4]$	β-PVDF/ $[C_6MIM][BF_4]$	β-PVDF/ $[C_8MIM][BF_4]$	β-PVDF/ $[C_{10}MIM][BF_4]$
1-C	−0.28164	−0.26384	−0.26397	−0.26407	−0.26417	−0.26371
2-C	0.270393	0.259017	0.258906	0.257909	0.258369	0.257652
3-C	−0.20113	−0.1676	−0.16876	−0.16897	−0.16902	−0.16905
4-C	0.273268	0.255673	0.256276	0.256013	0.255939	0.256099
5-C	−0.2031	−0.1849	−0.18293	−0.18272	−0.18306	−0.18306
6-C	0.270204	0.255602	0.259998	0.261484	0.261417	0.261551
7-C	−0.19749	−0.18904	−0.17961	−0.17854	−0.17868	−0.17831
8-C	0.201704	0.190685	0.192397	0.193384	0.194168	0.193168
9-F	−0.16975	−0.19573	−0.19353	−0.19347	−0.19395	−0.19406
10-F	−0.16975	−0.15358	−0.15637	−0.15486	−0.15511	−0.1539
11-F	−0.15488	−0.1756	−0.17087	−0.17051	−0.17104	−0.17028
12-F	−0.15488	−0.13724	−0.14289	−0.14285	−0.14224	−0.14257
13-F	−0.15456	−0.17034	−0.16713	−0.16755	−0.16772	−0.16719
14-F	−0.15456	−0.13555	−0.14135	−0.14262	−0.14229	−0.14329
15-F	−0.16766	−0.17008	−0.17412	−0.17384	−0.17391	−0.17307
16-F	−0.16766	−0.15797	−0.15361	−0.15448	−0.15489	−0.15545
17-H	0.117101	0.103585	0.104324	0.104251	0.104179	0.104103
18-H	0.113208	0.116682	0.116949	0.116833	0.116639	0.116328
19-H	0.113208	0.106063	0.105794	0.106085	0.106161	0.105583
20-H	0.116744	0.122905	0.124184	0.124374	0.123871	0.123732
21-H	0.116744	0.090341	0.088772	0.089001	0.08963	0.089286
22-H	0.11645	0.124034	0.124382	0.124173	0.124188	0.124148
23-H	0.11645	0.10256	0.09377	0.09296	0.093679	0.094077
24-H	0.12171	0.126215	0.128582	0.128226	0.128068	0.128139
25-H	0.12171	0.13071	0.113497	0.110871	0.110698	0.109662
26-H	0.109129	0.111438	0.115	0.112767	0.11214	0.113002

for atom numbers). Complete HOMO and LUMO composition of β-PVDF/IL systems are provided in Table S5 (a)–(e) Supplementary Information.

Different chemical parameters e.g., ionization energy, electron affinity, electronegativity, chemical potential, chemical hardness, chemical softness, electrophilicity index, derived from HOMO, LUMO energy values as described in Eqs. 6–10 are listed in Table 8 along with the mention of HOMO–LUMO energy gap. Pure β-PVDF possesses the highest E_{gap} and it reduces considerably when ionic liquids are added to it. This fact can be correlated to the increased ionic conductivity of PVDF with ionic liquid addition.[26,27,56,57] Interestingly, the E_{gap} values of ionic liquid added β-PVDF molecules are almost in the same range irrespective of the number of the carbon atoms in the alkyl chain present in the

Table 5. HOMO and LUMO compositions of pure β-PVDF and β-PVDF/IL systems, calculated using Hirschfeld orbital composition analysis algorithm in Multiwfn (atom numbers are given according to Figure 3(b)) [Calculation method: DFT-D; functional: B3LYP; basis set: 6-311+G(d,p)].

Atom number	Frontier Orbital Composition		Atom number	Frontier Orbital Composition	
	HOMO	LUMO		HOMO	LUMO
1(C)	4.41%	1.63%	14(F)	6.20%	1.34%
2(C)	5.23%	0.96%	15(F)	3.32%	0.84%
3(C)	7.98%	4.91%	16(F)	3.32%	0.84%
4(C)	7.41%	1.91%	17(H)	0.97%	0.32%
5(C)	9.18%	7.40%	18(H)	0.28%	2.31%
6(C)	6.62%	2.15%	19(H)	0.28%	2.31%
7(C)	6.54%	6.18%	20(H)	0.38%	7.29%
8(C)	4.06%	2.77%	21(H)	0.38%	7.29%
9(F)	4.37%	0.66%	22(H)	0.44%	10.72%
10(F)	4.37%	0.66%	23(H)	0.44%	10.72%
11(F)	7.19%	1.27%	24(H)	0.31%	9.05%
12(F)	7.19%	1.27%	25(H)	0.31%	9.05%
13(F)	6.20%	1.34%	26(H)	2.63%	4.75%

cation. However, ionic liquid added PVDF complexes are expected to have a higher viscosity than pure ionic liquid molecules, which should reduce the mobility of ion pairs resulting in decreasing ionic conductivity of the complex. But $[C_2MIM][BF_4]$ added β-PVDF system is found to show the lowest E_{gap} (6.72 eV), which is even lower than the E_{gap} values of all the pure ionic liquids reported in this study. Similar kind of observation, as reported by Shalu *et al.,*[53] demonstrated that small amount (∼10%) of PVDF addition within $[C_4MIM][BF_4]$ ionic liquid makes the conductivity of the system even higher than that in case of pristine $[C_4MIM][BF_4]$. HOMO–LUMO energy gap is directly proportional to the chemical hardness of a molecule. Higher chemical hardness implies higher chemical stability as they oppose charge transfer by opposing the change in electron density and distribution, in other words, reducing the polarizability of the molecules. Pure β-PVDF has a very high hardness (low softness) and chemical stability than ionic liquid added PVDF systems because of its high E_{gap} value as mentioned earlier. Addition of ionic liquids reduces the hardness of β-PVDF molecule and increases the polarizability, thereby enhancing the piezoelectric property. Among the ionic liquids discussed here, the lowest hardness (highest softness) value is found in case of $[C_{10}MIM][BF_4]$ and $[C_6MIM][BF_4]$ is found to show the highest hardness (lowest softness) value. On the contrary, $[C_{10}MIM][BF_4]$/β-PVDF and $[C_2MIM][BF_4]$/β-PVDF systems are found to possess the highest and the lowest hardness, respectively, among the other ionic liquid, added β-PVDF complexes discussed here as shown in Table 8.

3.6 *Molecular Electrostatic Potential*

Figure 6 represents the molecular electrostatic potential (MEP) plots of pure β-PVDF, pure ionic liquid $[C_{10}MIM][BF_4]$ and ionic liquid added β-PVDF system, namely, β-PVDF/$[C_{10}MIM][BF_4]$. MEP plots of the rest of the ILs and β-PVDF/IL systems are provided in Supplementary Figures S6 and S7, respectively. All the plots are formed by mapping the electrostatic potential of the systems onto their constant electron density surface (iso-value=0.0004). The different values of the electrostatic potential (ESP) at the surface are represented by different colours. Red parts of the surface refer to the sites for electrophilic reactions with negative ESP, blue parts represent nucleophilic sites with the positive ESP and the green parts correspond zero ESP, i.e, the neutral portions of the surface.[58] From Figure 6(a), it is evident that the hydrogen atoms present in the β-PVDF molecules are the most nucleophilic sites, which tend to interact with the electrophilic anion of the ionic liquid molecule. Figure 6(b) depicts that the carbon chain attached with the imidazolium ring of the cation of ionic liquids is associated with near zero ESP value.

3.7 *Natural Bond Orbital (NBO) analysis*

Although there is a considerable number of experimental findings available on qualitative description of the interaction between PVDF and ionic liquid molecules, no satisfactory quantitative analysis is found to describe which part of the polymer molecule interacts with which part of the ionic liquid (cation or anion). According to Wang *et al.,*[27] the interaction between the polymer

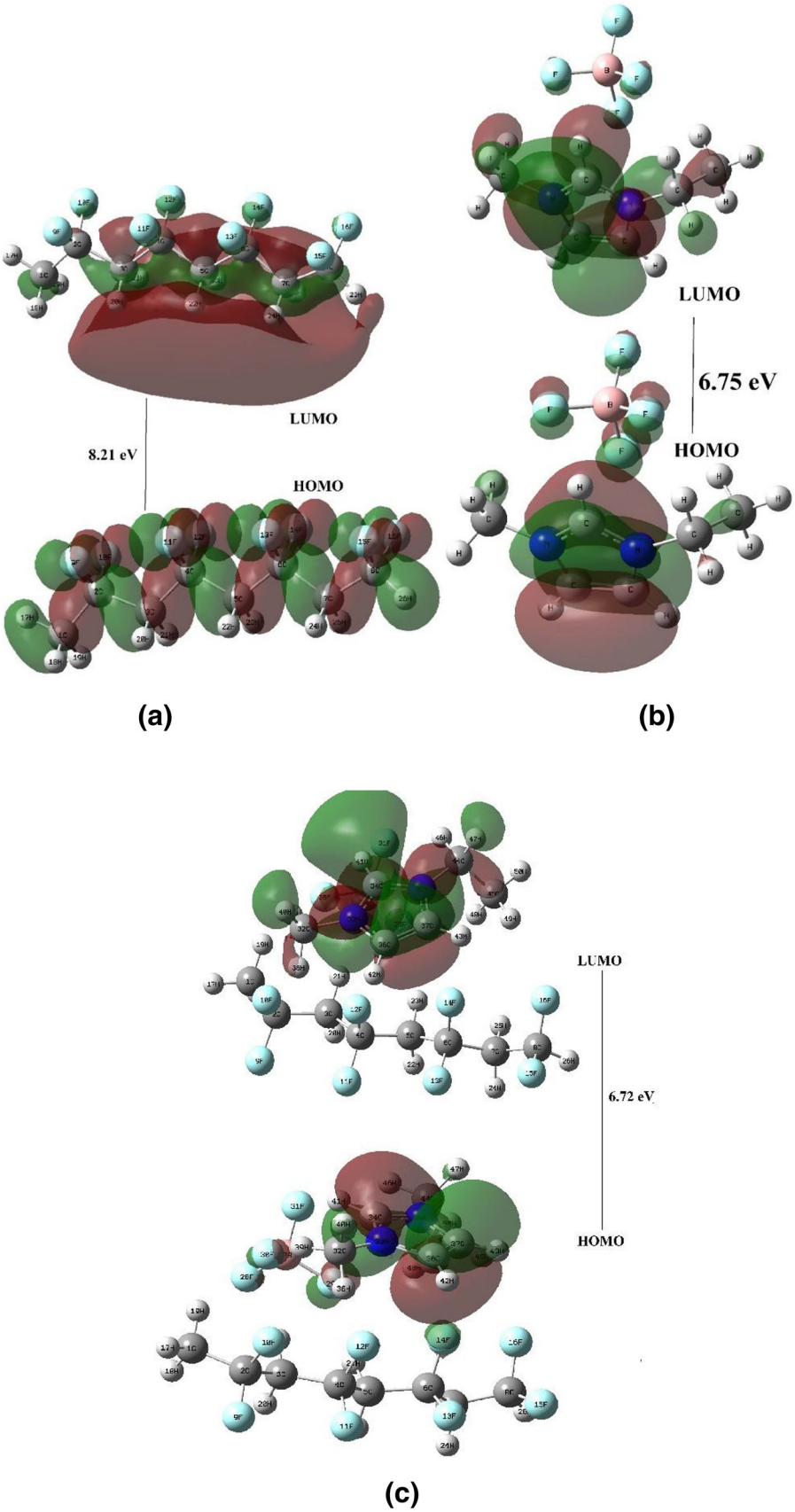

Figure 4. Positions of HOMO and LUMO in (a) β-PVDF, (b) [C_2MIM][BF_4], (c) β-PVDF/[C_2MIM][BF_4] [Method: DFT-D, functional: B3LYP, basis set: 6-311+G(d,p)].

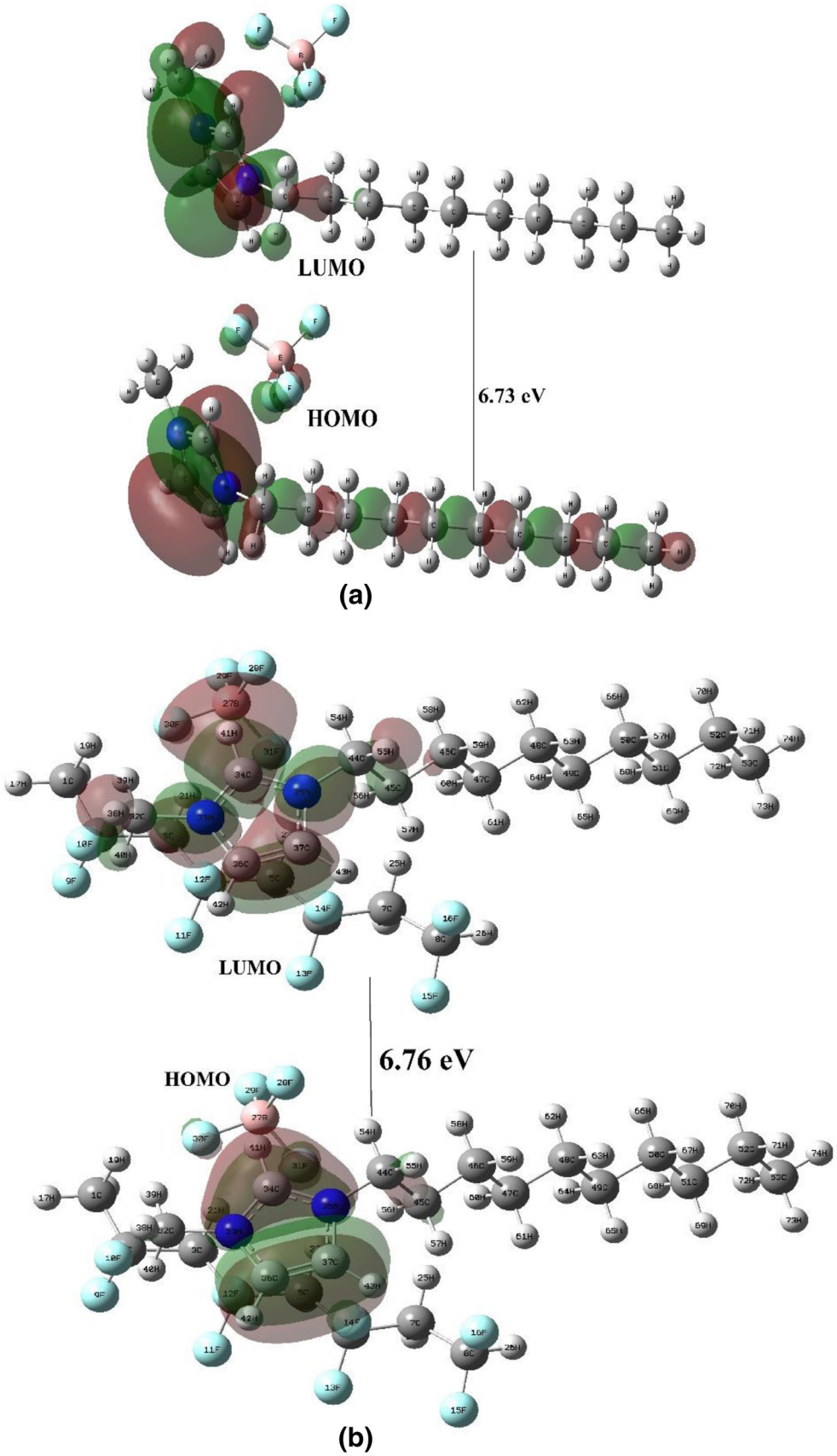

Figure 5. Positions of HOMO and LUMO in (a) $[C_{10}MIM][BF_4]$, (b) β-PVDF/$[C_{10}MIM][BF_4]$ [method: DFT-D, functional: B3LYP, basis set: 6-311+G(d,p)].

Table 6. Atoms with the largest contribution (>5%) to the HOMO in β-PVDF+IL systems (refer Figure 3(b) for atom numbers).

Atom	HOMO composition (%) of the system under study				
	β-PVDF/ $[C_2MIM][BF_4]$	β-PVDF/ $[C_4MIM][BF_4]$	β-PVDF/ $[C_6MIM][BF_4]$	β-PVDF/ $[C_8MIM][BF_4]$	β-PVDF/ $[C_{10}MIM][BF_4]$
33(N)	6.01%	5.89%	5.87%	5.85%	5.81%
34(C)	20.13%	20.15%	20.19%	20.17%	20.18%
35(N)	6.11%	6.18%	6.20%	6.22%	6.24%
36(C)	28.09%	28.39%	28.38%	28.33%	28.34%
37(C)	27.66%	27.51%	27.39%	27.34%	27.24%
Total	**88.00%**	**88.12%**	**88.03%**	**87.91%**	**87.81%**

Table 7. Atoms with the largest contribution (>5%) to the LUMO in β-PVDF+IL systems (refer Figure 3(b) for atom numbers).

Atom	LUMO composition (%) of the system under study				
	β-PVDF/ $[C_2MIM][BF_4]$	β-PVDF/ $[C_4MIM][BF_4]$	β-PVDF/ $[C_6MIM][BF_4]$	β-PVDF/ $[C_8MIM][BF_4]$	β-PVDF/ $[C_{10}MIM][BF_4]$
33(N)	15.05%	15.67%	15.69%	15.64%	15.78%
34(C)	33.14%	34.02%	34.04%	34.03%	34.14%
35(N)	15.31%	15.68%	15.71%	15.71%	15.73%
37(C)	5.26%	5.15%	5.13%	5.16%	5.09%
41(C)	6.62%	6.49%	6.44%	6.48%	6.43%
Total	**75.38%**	**77.01%**	**76.61%**	**77.02%**	**77.17%**

Table 8. Different chemical parameters obtained from HOMO LUMO energies.

System	Ionization energy (IE) (eV)	Electron affinity (EA) (eV)	Electro negativity (χ) (eV)	Chemical potential (μ) (eV)	Chemical Hardness (η)	Chemical softness (S)	Electro philicity index (ω)	Egap energy (eV)
β-PVDF (C_S symmetry)	8.96412	0.748575	4.856347	−4.85635	4.107773	0.243441	2.870669	8.215545
β-PVDF (C_1 symmetry)	9.00548	0.689527	4.847504	−4.8475	4.157977	0.240502	2.825688	8.315954
$[C_2MIM][BF_4]$	8.110239	1.357557	4.733898	−4.7339	3.376341	0.296179	3.31865	6.752682
$[C_4MIM][BF_4]$	8.083844	1.334972	4.709408	−4.70941	3.374436	0.296346	3.286256	6.748872
$[C_6MIM][BF_4]$	8.082483	1.326808	4.704646	−4.70465	3.377837	0.296047	3.276311	6.755675
$[C_8MIM][BF_4]$	8.076769	1.330618	4.703693	−4.70369	3.373076	0.296465	3.279608	6.746151
$[C_{10}MIM][BF_4]$	8.06398	1.329257	4.696619	−4.69662	3.367361	0.296968	3.275298	6.734723
β-PVDF/$[C_2MIM][BF_4]$	7.8667	1.14395	4.505325	−4.50533	3.361375	0.297497	3.019294	6.72275
β-PVDF/$[C_4MIM][BF_4]$	7.957857	1.194563	4.57621	−4.57621	3.381647	0.295714	3.096375	6.763294
β-PVDF/$[C_6MIM][BF_4]$	7.960034	1.194835	4.577434	−4.57743	3.382599	0.295631	3.09716	6.765199
β-PVDF/$[C_8MIM][BF_4]$	7.948877	1.186672	4.567775	−4.56777	3.381103	0.295761	3.085467	6.762206
β-PVDF/$[C_{10}MIM][BF_4]$	7.949149	1.182046	4.565598	−4.5656	3.383552	0.295547	3.080296	6.767104

matrix and ionic liquid second phase basically occurs through the anion of the IL and hydrogen atoms of PVDF. On the contrary, Liang *et al.,*[59] have demonstrated that the positive ion of the ionic liquid plays the major role of interaction with the PVDF molecule. The present study provides a quantitative description of this phenomenon with the help of NBO analysis which is based on second-order perturbation theory and quantifies the extent of intra-unit and inter-unit electron delocalization of a molecular complex by the magnitude of the corresponding stabilization energy ($E^{(2)}$) values. The higher the stabilization energy, the greater is the electron delocalization. In the present study, unit 1, 2 and 3 refer to the PVDF, anionic and the cationic portions of the ionic liquids, respectively. From inter-unit NBO interaction, as presented in the supplementary Table S6

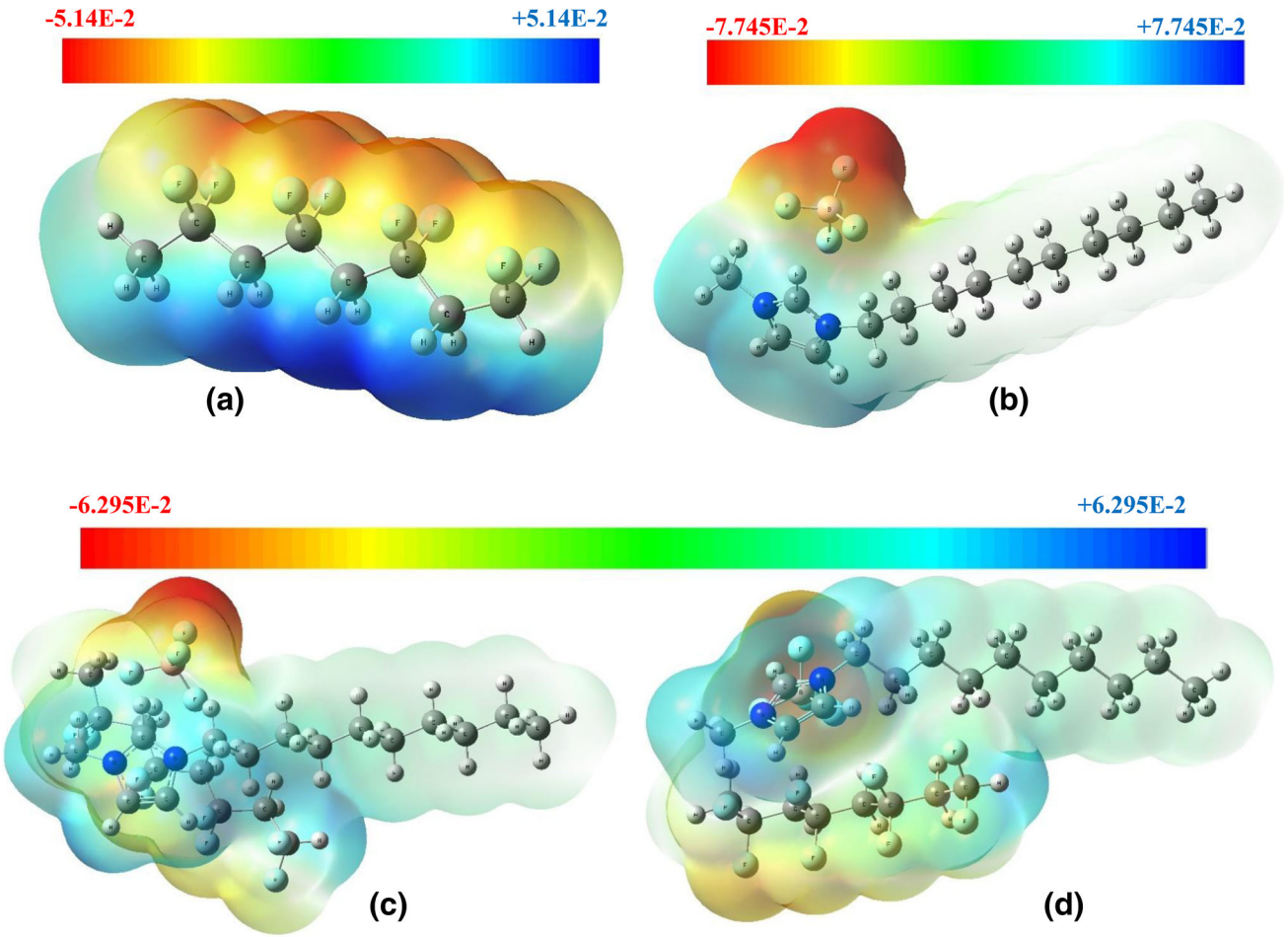

Figure 6. MEP plot of (a) β-PVDF, (b) $[C_{10}MIM][BF_4]$, (c) and (d) β-PVDF/ $[C_{10}MIM][BF_4]$ viewed from two direction for better understanding [method: DFT-D, functional: B3LYP, basis set: 6-311+G(d,p)].

and Table S7, it is evident that both the cation and anion of the ionic liquid molecules interact considerably with the PVDF molecules. The maximum $E^{(2)}$ value corresponding to inter-unit electron delocalization is in the range of 1.5 kcal/mol for PVDF–IL anion (unit 1 and 2) and 0.5 kcal/mol for PVDF–IL cation (unit 1 and 3) NBO interaction (Tables S6 and S7). However, it is observed that the intra-unit interaction is much greater than the inter-unit interaction, which depicts that the electron delocalization is much higher within one unit than among different units. The stabilization energy values as listed within unit 1, i.e., pure β-PVDF part of the complex (Tables 9, 10, 11), show that the extent of electron delocalization within lone pairs of F atoms and antibonding orbital of C–F bonds reduces as the ionic liquid is added to pure β-PVDF. However, the variation of NBO interaction energies is observed to be independent of alkyl chain length of the cation of ionic liquid (unit 3). Charge transfer from πC36-C37‡ to LP N35‡for all the complexes presented here are found to be associated with the highest stabilization energy of 250 kcal/mol (for pure β-PVDF) and 260 kcal/mol (for β-PVDF+IL complexes). (‡ *refer Figure 3 for atom numbers*). And that from LP N35‡ to π*N33-C34 corresponds to the second highest stabilization energy of 80 kcal/mol (for pure β-PVDF as well as for β-PVDF+IL complexes) which depicts high electron delocalization in the donor NBOs resulting in weakening of the bonds.

3.8 *Simulating β-PVDF within the ionic liquid solvent continuum*

So far all the systems (PVDF, IL, and PVDF/IL) are analysed as isolated systems to elucidate the intra and inter-molecular interactions. But it can be questioned whether these systems can be explained considering the PVDF molecule within the ionic liquid solvent continuum. An individual β-PVDF molecule within $[C_4MIM][BF_4]$ solvent continuum is optimized using the solvation model based on density (SMD) computational approach.[49,50] Optimized geometry of β-PVDF in the solvated phase is provided in supplementary Figure

Table 9. NBO analysis of pure and IL added β-PVDF systems *within unit 1 (PVDF part)* (refer Figure 3(b) for atom numbers).

Donor NBO	Type	Acceptor NBO	Type	Stabilization energy ($E^{(2)}$) (kcal/mol)					
				Pure β-PVDF	β-PVDF/ [C_2MIM] [BF_4]	β-PVDF/ [C_4MIM] [BF_4]	β-PVDF/ [C_6MIM] [BF_4]	β-PVDF/ [C_8MIM] [BF_4]	β-PVDF/ [C_{10}MIM] [BF_4]
LP F9	n	BD* C2-F10	σ*	16.46	14.91	14.99	15.01	14.96	14.95
LP F10	n	BD* C2-F9	σ*	16.46	14.40	14.34	14.32	14.36	14.36
LP F11	n	BD* C4-F12	σ*	16.72	15.54	15.88	15.91	15.87	15.92
LP F12	n	BD* C4-F11	σ*	16.72	14.60	14.34	14.35	14.37	14.36
LP F13	n	BD* C6-F14	σ*	16.75	15.64	15.93	15.91	15.90	15.91
LP F14	n	BD* C6-F13	σ*	16.75	14.99	14.79	14.81	14.82	14.82
LP F15	n	BD* C8-F16	σ*	15.67	15.18	15.34	15.31	15.30	15.34
LP F16	n	BD* C8-F15	σ*	15.67	14.11	14.04	14.05	14.09	14.06

Table 10. NBO analysis of pure and IL added β-PVDF systems *within unit 2 (anionic part of IL)* (refer Figure 3(b) for atom numbers).

Donor NBO	Type	Acceptor NBO	Type	Stabilization energy ($E^{(2)}$)(kcal/mol)				
				β-PVDF/ [C_2MIM] [BF_4]	β-PVDF/ [C_4MIM] [BF_4]	β-PVDF/ [C_6MIM] [BF_4]	β-PVDF/ [C_8MIM] [BF_4]	β-PVDF/ [C_{10}MIM] [BF_4]
LP F28	n	RY* B27		10.55	10.51	10.38	10.54	10.43
LP F28	n	BD* B27-F29	σ*	11.34	11.09	11.12	11.09	11.07
LP F28	n	BD* B27-F31	σ*	13.65	10.87	10.87	10.86	10.89
LP F29	n	BD* B27-F30	σ*	10.76	11.88	12.37	11.98	12.20
LP F30	n	BD* B27-F29	σ*	11.28	13.83	13.67	13.76	13.73
LP F31	n	BD* B27-F29	σ*	10.24	10.91	10.89	11.13	11.21
LP 31	n	BD* B27-F28	σ*	11.39	10.10	10.09	10.10	10.06

Table 11. NBO analysis of pure and IL added β-PVDF systems *within unit 3 (cationic part of IL)* (refer Figure 3(b) for atom numbers).

Donor NBO	Type	Acceptor NBO	Type	Stabilization energy ($E^{(2)}$)(kcal/mol)				
				β-PVDF/ [C_2MIM] [BF_4]	β-PVDF/ [C_4MIM] [BF_4]	β-PVDF/ [C_6MIM] [BF_4]	β-PVDF/ [C_8MIM] [BF_4]	β-PVDF/ [C_{10}MIM] [BF_4]
BD N33-C34	π	LP N35	n	21.39	21.32	21.32	21.37	21.34
BD N33-C34	π	BD* C36-C37	π*	17.23	17.14	17.13	17.16	17.14
BD C36-C37	π	LP N35	n	251.86	261.31	259.05	260.06	259.63
BD C36-C37	π	BD* N33-C34	π*	13.73	13.73	13.74	13.72	13.73
LP N35	n	BD* N33-C34	π*	80.80	80.29	80.30	80.25	80.27
LP N35	n	BD* C36-C37	π*	30.58	30.40	30.45	30.39	30.42
BD N33-C34	π	BD* C36-C37	π*	18.67	18.36	18.42	18.41	18.40

S8 (Supplementary Information). The solvation energy value ($\Delta E_{solvation} = E_{insolution} - E_{ingasphase}$) is found as −78.24 kJ/mol suggesting the stability of β-PVDF within IL continuum. If we compare the geometry with that in the gas phase (ref. Figure 1 (b)), no satisfactory structural change is observed, but dipole moment value is found to increase from 8.7310 D to 12.3964 D upon solvation. This significant increase in the dipole moment

value results from the additional dipole moment induced by the reaction field of the solvent continuum.[39] Thus, this model cannot explain well ion–dipole interaction occurring within the systems [ref. Section 3.1 and 3.3]. Besides, a HOMO–LUMO gap of the solvated molecule is found to increase upon solvation, as compared to that in the gas phase [E_{gap} value is 8.22 eV in the gas phase and 8.69 eV in the solution phase, ref. Figure 4(a) for the gas phase and Figure S9 (Supplementary Information) for solution phase]. But the addition of ionic liquid is supposed to increase the ionic conductivity of the system [as explained in section 3.5], i.e., HOMO LUMO gap should decrease. So this model has not found to be suitable to explain the present system under study. However, the effect of the polar aprotic solvents used in the synthesis of PVDF/IL composite (e.g., n, n-dimethylformamide or DMF) on the DFT calculations has found to be quite relevant which we are going to explain in our next article.

4. Conclusions

Density functional theory studies are carried out for four monomer units of pristine and IL added alpha and beta PVDF. Dispersion-corrected restricted B3LYP exchange-correlation density functional is found to be the most reliable as it optimizes the systems understudy to the least energy configurations. Ionic liquid addition changes the symmetry of β-PVDF structure from C_S to C_1. Pure β-PVDF possess higher dipole moment than pure α-PVDF which makes the former more electroactive. The magnitudes of the dipole moment are almost constant with the chain length of the cation of the ionic liquid. Overall interaction between PVDF and ionic liquid molecules are quantified by interaction energy calculations, which suggest a better interaction of the ionic liquids with β-PVDF than with α-PVDF. The individual contribution of cations and anions of ionic liquids to the total interaction within PVDF/IL complexes are demonstrated using NBO analysis. Intra-unit electron delocalization is found to be greater than inter-unit electron delocalization. Mulliken population analysis (MPA) and atomic dipole moment corrected Hirschfeld (ADCH) population analysis have been carried out to quantify the charge distribution within all the systems under study. The charge distribution within a pristine β-PVDF molecule has not been found to vary much after ionic liquid addition. Chemical reactive properties of the systems under study are described using HOMO–LUMO theory. HOMO–LUMO energy gaps (E_{gap}) of the systems are found to decrease with the addition of ionic liquids thereby increasing the ionic conductivity. However, this simulation approach discussed here has the limitation of not obtaining satisfactory results for bulk systems. To find out the bulk properties of the systems under study, we are performing solid-state DFT calculations using plane wave basis sets and molecular dynamics (MD) simulations and the work is under progress.

Supplementary Information (SI)

Detailed structural information including total energy, dipole moment and mean polarizability values for all the systems under study are provided in the supplementary information. Besides, Mulliken and ADCH population analyses for all the systems using different computation methods are given. Images of HOMO–LUMO distribution are represented along with complete HOMO–LUMO composition analysis. Inter-unit NBO interactions are provided for the β-PVDF/IL systems. In the end, optimized geometry and HOMO–LUMO distribution of a β-PVDF molecule within [C_4MIM][BF_4] continuum are provided. Supplementary Information is available at www.ias.ac.in/chemsci.

References

1. Martins P and Lanceros-Méndez S 2013 Polymer-based magnetoelectric materials *Adv. Funct. Mater.* **23** 3371
2. Mai M, Ke S, Lin P and Zeng X 2015 Ferroelectric polymer thin films for organic electronics *J. Nanomater.* **2015** 1
3. Martins P, Lopes A C and Lanceros-Mendez S 2014 Electroactive phases of poly(vinylidene fluoride): Determination, processing and applications *Prog. Polym. Sci.* **39** 683
4. Poulsen M and Ducharme S 2010 Why Ferroelectric Polyvinylidene Fluoride is Special Why Ferroelectric Polyvinylidene Fluoride is Special *IEEE Trans. Dielectr. Electr. Insul.* **17** 1028
5. Itoh A, Takahashi Y, Furukawa T and Yajima H 2014 Solid-state calculations of poly(vinylidene fluoride) using the hybrid DFT method: Spontaneous polarization of polymorphs 2014 *Polym. J.* **46** 207
6. Lines M E and Glass A M 1977 In *Principles and Applications of Ferroelectrics and Related Materials* 1st edn. (Oxford: Clarendon)
7. Dias J C, Martins M S, Ribeiro S, Silva M M, Esperança J M S S, Ribeiro C, Botelho G, Costa C M and Lanceros-Mendez S 2016 Electromechanical actuators based on poly(vinylidene fluoride) with [$N_{1\,1\,1\,2(OH)}$][NTf_2] and [C2mim] [C_2SO_4] *J. Mater. Sci.* **51** 9490
8. Ramer N J and Stiso K A 2005 Structure and Born effective charge determination for planar-zigzag β-poly(vinylidene fluoride) using density-functional theory *Polym. J.* **46** 10431
9. Li Z, Wang J, Wang X, Yang Q and Zhang Z 2015 Ferro- and piezo-electric properties of a poly(vinyl fluoride) film with high ferro- to para-electric phase transition temperature *RSC Adv.* **5** 80950
10. Wang Z Y, Fan H Q, Su K H, Wang X and Wen Z Y 2007 Structure, phase transition and electric properties

of poly(vinylidene fluoride-trifluoroethylene) copolymer studied with density functional theory *Polym. J.* **48** 3226
11. Bohlé M and Bolton K 2014 Conformational studies of poly(vinylidene fluoride), poly(trifluoroethylene) and poly(vinylidene fluoride-co-trifluoroethylene) using density functional theory *Phys. Chem. Chem. Phys.* **16** 12929
12. Gomes J, Nunes J S, Sencadas V and Lanceros-Mendez S 2010 Influence of the β-phase content and degree of crystallinity on the piezo-and ferroelectric properties of poly(vinylidene fluoride) *Smart Mater. Struct*. **19** 1
13. Nabata Y 1990 Structure of crosslinked poly (vinylidene fluoride) crystallized from melt under uniaxial compression *Jpn. J. Appl. Phys.* **29** 1298
14. Qian X, Wu S, Furman E, Zhang Q and Su J 2015 Ferroelectric polymers as multifunctional electroactive materials: Recent advances, potential, and challenges *MRS Comm.* **5** 115
15. Abolhasani M M, Zarejousheghani F, Cheng Z X and Naebe M 2015 A facile method to enhance ferroelectric properties in PVDF nanocomposites *RSC Adv.* **5** 22471
16. Mofokeng T G, Luyt A S, Pavlovic V P, Pavlovic V B, Dudic D, Vlahovic B and Djokovic V 2014 Ferroelectric nanocomposites of polyvinylidene fluoride/polymethyl methacrylate blend and $BaTiO_3$ particles: Fabrication of β-crystal polymorph rich matrix through mechanical activation of the filler *J. Appl. Phys.* **115** 1
17. Mahdi R I, Gan W C, Halim N A, Velayutham T S and Majid W H A 2015 Ferroelectric and pyroelectric properties of novel lead-free polyvinylidenefluoride-trifluoroethylene-$Bi_{0.5}Na_{0.5}TiO_3$ nanocomposite thin films for sensing applications *Ceram. Int.* **41** 13836
18. Alomari A, Batra A K and Arjun K J 2016 Optical and electronic characterization of P(VDF-TrFE)/La_2O_3 nanocomposite films *Optik* **127** 10335
19. Lee W G, Park B E and Park K E 2013 Ferroelectric properties of the organic films of poly(vinylidene fluoride-trifluoroethylene blended with inorganic Pb(Zr, Ti)O_3 *Thin Solid Films* **546** 171
20. Xia W, Xu Z, Wen F and Zhang Z 2012 Electrical energy density and dielectric properties of poly(vinylidene fluoride-chlorotrifluoroethylene)/$BaSrTiO_3$ nanocomposites *Ceram. Int.* **38** 1071
21. Chan H L W, Chan W K, Zhang Y and Choy C L 1998 Pyroelectric and piezoelectric properties of lead titanate/polyvinylidene fluoride-trifluoroethylene 0-3 composites *IEEE Trans. Dielectr. Electr. Insul.* **5** 505
22. Fang M, Wang Z, Li H and Wen Y 2015 Fabrication and dielectric properties of $Ba(Fe_{0.5}Nb_{0.5})O_3$/poly(vinylidene fluoride) composites *Ceram. Int.* **117** 1
23. Thakur P, Kool A, Bagchi B, Hoque N A, Das S and Nandy P 2015 The role of cerium nitrate hexahydrate salts on electroactive β phase nucleation and dielectric properties of poly(vinylidene fluoride) thin films *RSC Adv*. **5** 28487
24. Xing C, You J, Li Y and Li J 2015 Nanostructured Poly(vinylidene fluoride)/Ionic Liquid Composites: Formation of Organic Conductive Nanodomains in Polymer Matrix *J. Phys. Chem. C* **119** 21155
25. Dias J C, Lopes A C, Magalhães B, Botelho G, Silva M M, Esperança J M S S and Lanceros-Mendez S 2015 High performance electromechanical actuators based on ionic liquid/poly(vinylidene fluoride) *Polym. Test.* **48** 199
26. Mejri R, Dias J C, Lopes A C, Bebes Hentati S, Silva M M, Botelho G, Mão De Ferro A, Esperança J M S S, Maceiras A, Laza J M, Vilas J L, León L M and Lanceros-Mendez S 2015 Effect of ionic liquid anion and cation on the physico-chemical properties of poly(vinylidene fluoride)/ionic liquid blends *Eur. Polym. J.* **71** 304
27. Wang F, Lack A, Xie Z, Frübing P, Taubert A and Gerhard R 2012 Ionic-liquid-induced ferroelectric polarization in poly(vinylidene fluoride) thin films *Appl. Phys. Lett.* **100** 1
28. Pal S and Kundu T K 2013 DFT-based inhibitor and promoter selection criteria for pentagonal dodecahedron methane hydrate cage *J. Chem. Sci.* **125** 1259
29. Pal S and Kundu T K 2013 Stability analysis and frontier orbital study of different glycol and water complex *ISRN Phys. Chem.* **2013** 1
30. Frisch M J *et al.* 2010 Gaussian 09 Revision (B.01) (Gaussian Inc. Wallingford CT)
31. Foresman J B, Frisch A E and Gaussin, Inc. 1996 In *Exploring Chemistry with Electronic Structure Methods* 2nd edn. (Gaussian, Inc., Pittsburgh, PA)
32. Grimme S 2011 Density functional theory with London dispersion correction *WIREs Comput. Mol. Sc.* **1** 211
33. Becke A D 1993 A new mixing of Hartree–Fock and local density-functional theories *J. Chem. Phys.* **98** 1372
34. Lee C, Yang W and Parr R G 1988 Development of the Colle-Salvetti correlation-energy formula into a functional of the electron density *Phys. Rev. B* **37** 785
35. Perdew J P and Yue W 1986 Accurate and simple density functional for the electronic exchange energy: Generalized gradient approximation *Phys. Rev. B* **33** 8800
36. Walker M, Harvey A J A, Sen A and Dessent C E H 2013 Performance of M06, M06-2X, and M06-HF density functionals for conformationally flexible anionic clusters: M06 functionals perform better than B3LYP for a model system with dispersion and ionic hydrogen-bonding interactions *J. Phys. Chem. A* **117** 12590
37. Chai J D and Head-Gordon M 2008 Long-range corrected hybrid density functionals with damped atom–atom dispersion corrections *Phys. Chem. Chem. Phys.* **10** 6615
38. Řezáč J and Hobza P 2016 Benchmark Calculations of Interaction Energies in Noncovalent Complexes and Their Applications *Chem. Rev.* **116** 5038
39. Levine I N 2012 In *Quantum Chemistry* 7th edn. (Pearson: New York)
40. Mulliken R S 1955 Electronic Population Analysis on LCAO-MO Molecular Wave Functions. IV. Bonding and Antibonding in LCAO and Valence-Bond Theories *J. Chem. Phys.* **23** 2343
41. Hirshfeld F L 1977 Bonded-atom fragments for describing molecular charge densities *Theor. Chim. Acta* **44** 129
42. Lu T and Chen F 2012 Atomic Dipole Moment Corrected Hirshfeld Population Method *J. Theor. Comput. Chem.* **11** 163
43. Lu T and Chen F 2012 Multiwfn: A multifunctional wavefunction analyzer *J. Comput. Chem.* **33** 580
44. Solymar L and Walsh D 2004 In *Electrical Properties of Materials* 7th edn. (Oxford: Clarendon)

45. Zhan C G, Nichols J A and Dixon D A 2003 Ionization potential, electron affinity, electronegativity, hardness, and electron excitation energy: Molecular properties from density functional theory orbital energies *J. Phys. Chem. A* **107** 4184
46. Parr R and Yang W 1989 In *Density-functional theory of atoms and molecules* 1st edn. (Oxford: Clarendon)
47. Gázquez J L 1993 Hardness and Softness in Density Functional Theory *Structure and Bonding* **80** 27
48. Parr R G, Szentpály L V and Liu S 1999 Electrophilicity index *J. Am. Chem. Soc.* **121** 1922
49. Marenich A V, Cramer C J and Truhlar D G 2009 Universal solvation model based on solute electron density on a continuum model of the solvent defined by the bulk dielectric constant and atomic surface tensions *J. Phys. Chem. B* **113** 6378
50. Bernales V S, Marenich A V, Contreras R and Cramer C J 2012 Quantum mechanical continuum solvation models for ionic liquids *J. Phys. Chem. B* **116** 9122
51. Hasegawa R, Takahashi Y, Chatani Y and Tadokoro H 1971 Crystal Structures of Three Crystalline Forms of Poly(vinylidene fluoride) *Polym. J.* **3** 600
52. Pilli S R, Banerjee T and Mohanty K 2015 HOMO-LUMO energy interactions between endocrine disrupting chemicals and ionic liquids using the density functional theory: Evaluation and comparison *J. Mol. Liq.* **207** 112
53. Shalu, Chaurasia S K, Singh R K and Chandra S 2013 Thermal stability, complexing behavior, and ionic transport of polymeric gel membranes based on polymer PVdF-HFP and ionic liquid, [BMIM][BF4] *J. Phys. Chem. B* **117** 897
54. Wang Z Y, Fan H Q, Su K H and Wen Z Y 2006 Structure and piezoelectric properties of poly(vinylidene fluoride) studied by density functional theory *Polymer J.* **47** 7988
55. Bultinck P, Van Alsenoy C, Ayers P W and Carbó-Dorca R 2007 Critical analysis and extension of the Hirshfeld atoms in molecules *J. Chem. Phys.* **126** 144111
56. Mejri R, Dias J C, Besbes Hentati S, Botelho G, Esperança J M S S, Costa C M and Lanceros-Mendez S 2016 Imidazolium-based ionic liquid type dependence of the bending response of polymer actuators *Eur. Polym. J.* **85** 445
57. Soares B G, Pontes K, Marins J A, Calheiros L F, Livi S and Barra G M O 2015 Poly(vinylidene fluoride-co-hexafluoropropylene)/polyaniline blends assisted by phosphonium - Based ionic liquid: Dielectric properties and β-phase formation *Eur. Polym. J.* **73** 65
58. Politzer P, Laurence P R and Jayasuriya K 1985 Molecular electrostatic potentials: An effective tool for the elucidation of biochemical phenomena *Environ. Health Perspect.* **61** 191
59. Liang C L, Mai Z H, Xie Q, Bao R Y, Yang W, Xie B H and Yang M B 2014 Induced formation of dominating polar phases of poly(vinylidene fluoride): Positive ion-CF_2 Dipole or Negative Ion-CH_2 dipole interaction *J. Phys. Chem. B* **118** 9104